Original Article
http://dx.doi.org/10.5115/acb.2011.44.4.274
pISSN 2093-3665 eISSN 2093-3673
Anatomy & Cell Biology acb

Morphological evidences in circumvallate papilla and von Ebners' gland development in mice

Wern-Joo Sohn[1], Gi-Jeong Gwon[2], Chang-Hyeon An[3], Cheil Moon[4], Yong-Chul Bae[4], Hitoshi Yamamoto[5], Sanggyu Lee[1], Jae-Young Kim[2]

[1]School of Life Science and Biotechnology, Departments of [2]Biochemistry, [3]Oral and Maxillofacial Radiology, and [4]Anatomy and Neuroscience, Institute for Hard Tissue and Bio-tooth Regeneration, School of Dentistry, Kyungpook National University, Daegu, Korea, [5]Dental Education Development Center, Tokyo Dental College, Chiba, Japan

Abstract: In rodents, the circumvallate papilla (CVP), with its underlying minor salivary gland, the von Ebners' gland (VEG), is located on the dorsal surface of the posterior tongue. Detailed morphological processes to form the proper structure of CVP and VEG have not been properly elucidated. In particular, the specific localization patterns of taste buds in CVP and the branching formation of VEG have not yet been elucidated. To understand the developmental mechanisms underlying CVP and VEG formation, detailed histological observations of CVP and VEG were examined using a three-dimensional computer-aided reconstruction method with serial histological sections and pan-Cytokeratins immunostainings. In addition, to define the developmental processes in CVP and VEG formation, we examined nerve innervations and cell proliferation using microinjections of AM1-43 and immunostainings with various markers, including phosphoinositide 3-kinase, Ki-67, PGP9.5, and Ulex europaeus agglutinin 1 (UEA1). Results revealed specific morphogenesis of CVP and VEG with nerve innervations patterns, evaluated by the coincided localization patterns of AM1-43 and UEA1. Based on these morphological and immunohistochemical results, we suggest that nerve innervations and cell proliferations play important roles in the positioning of taste buds in CVP and branching morphogenesis of VEG in tongue development.

Key words: Circumvallate papilla, von Ebners glands, Epithelial differentiation, AM1-43 microinjections, 3D computer-aided reconstruction

Received August 24, 2011; 1st Revised October 27, 2011, 2nd Revised November 9, 2011; Accepted November 14, 2011

Introduction

In rodents, there are three types of gustatory papillae including fungiform, foliate, and circumvallate. These gustatory papillae contain taste buds, which sense taste, with specific localization patterns [1]. Because of taste buds, gustatory papillae are distinguished from tongue oral epithelium, including filiform papillae. The circumvallate papilla (CVP), one of the gustatory papillae, contains taste buds with the specific localization pattern in the lateral trench wall regions. It has a tubulo-acinar salivary gland, the von Ebners' gland (VEG), which is composed of serous cells. In mice, there is one CVP in the middle one-third of the posterior tongue, which contains over two hundred taste buds in the trench wall of the papilla epithelium [2]. This CVP is well-studied and the physiological functions of taste sensations and developmental mechanisms in epithelial differentiation

Corresponding author:
Jae-Young Kim
Department of Biochemistry, School of Dentistry, IHBR, Kyungpook National University, 101 Dongin-dong 2-ga, Jung-gu, Daegu 700-422, Korea
Tel: +82-53-420-4998, Fax: +82-53-421-4276, E-mail: jykim91@knu.ac.kr

have been defined [1, 3].

During mice embryogenesis, after the epithelial invaginations of CVP, the formation of VEG is initiated underlying CVP through epithelial cell proliferations [4]. VEG has specific morphological and functional features that differ from those of other types of minor glands [2]. The VEG drains its serous contents into the deep groove at the periphery of CVP, which has numerous taste buds [5]. VEG was described as a gland involved in the simple washing of the trench surrounding the CVP and in producing digestive enzymes, particularly lipases, which are important mainly in the neonatal period when the pancreas is still immature [6, 7]. The CVP and VEG form a complex structure for physiological and functional unit for tasting and digestion [8]. To understand the function of the CVP and VEG complex, we examined the detailed morphogenesis of CVP and VEG using a three-dimensional (3D) computer-aided reconstructions method at embryonic day 16 (E16) and postnatal day three (PN3), since these developmental stages showed the most obvious morphological alterations during tongue development [4, 9]. The specific localization patterns of taste buds in the lateral trench wall of the CVP and the structural formation of VEG are governed by the developmental mechanisms of cellular events and molecular signaling [10-13]. Previous reports showed the important roles of nerve innervations in taste bud formation and epithelial differentiation [14-17]. In CVP and VEG development, specific nerve innervation patterns were examined using various nerve specific markers [18, 19]. However, these studies could not elucidate the precise localization of nerve innervations with the activity. In this study, a specialized pattern of nerve innervations and their activity was examined using AM1-43 microinjections to reveal developmental mechanisms in taste bud formation in CVP and branching morphogenesis of VEG.

Materials and Methods

All experiments were performed according to the guidelines of the Kyungpook National University, School of Dentistry, Intramural Animal Use and Care Committee.

Animals

Adult ICR mice were housed in a temperature-controlled room (22°C) under artificial illumination (lights on from 05:00 to 17:00), at 55% relative humidity, with free access to food and water. Mouse embryos were obtained from time-mated pregnant mice. The day on which a vaginal plug was confirmed was designated as E0.

Histology and immunohistochemistry

Sections were routinely stained with hematoxylin and eosin and evaluated by light microscopy. Specimens were fixed in 4% paraformaldehyde in phosphate-buffered saline overnight at 4°C, embedded in paraffin wax using conventional methods, and then cut to a thickness of 5 μm. Primary antibodies used were Ki-67 (cat. no. RM-9106, Thermo Scientific, Fremont, CA, USA), pan-Cytokeratins (cat. no. MS-343, Thermo Scientific), phosphoinositide 3-kinase (PI3K; cat. no. 04-403, Millipore, Bedford, MA, USA), Ulex europaeus agglutinin 1 (UEA1; cat. no. U1500-50A, USbio, Swampscott, MA, USA), and PGP9.5 (cat. no. ab8189, Abcam, Cambridge, MA, USA). Secondary antibodies used were of biotinylated goat, anti-rabbit, or anti-mouse IgG. The binding of the primary antibody to the sections was visualized using a diaminobenzidine tetrahydrochloride (DAB) reagent kit (cat. no. 00-2014, Zymed, San Francisco, CA, USA).

Three-dimensional reconstruction

All sections immunostained with pan-Cytokeratins were photographed using a DM2500 microscope (Leica, Wetzlar, Germany) and digital CCD camera (DFC420C, Leica). Two or three tongues were reconstructed from each specimen. Reconstruction software, which can be downloaded from http://synapses.clm.utexas.edu/tools/reconstruct/reconstruct.stm (August 20, 2007), was used to produce 3D images of all of the components of the CVP and VEG. Images were aligned automatically and manually using the software. Every image of the CVP and VEG was used for reconstruction. Thus, the actual reconstructed thickness was 10 μm.

Microinjections of AM1-43

After anesthetizing pregnant mice at E15 with Zoleltil and Rumpun, embryonic *in utero* microinjections of 1 μl AM1-43 (cat. no. 70024, Biotium Inc., Hayward, CA, USA) per embryo were performed as per previous reports [20-22]. The concentration of AM1-43 was 1 mg/ml. Intraperitoneal injections of 1 μl AM1-43 were also performed on new born mice at PN2. Twenty-four hours after the injections of AM1-43, the specimens were sacrificed and visualized under a fluorescent microscope (MZ-16FA, Leica). For histological observations, frontal frozen sections were performed at 20

http://dx.doi.org/10.5115/acb.2011.44.4.274

μm thickness. After observation, the same slides were used for immunohistochemistry to observe the co-localization patterns of UEA1 and PGP9.5.

Results

Morphogenesis of CVP and VEG in mice embryogenesis

To evaluate detailed morphological changes of CVP and VEG, we employed a 3D computer-aided reconstruction method after the frontal serial sections and the pan-Cytokeratins immunostainings of developing tongues. Dramatic morphological alterations of CVP and VEG have been observed at E16 and PN3 [12]. Therefore, we evaluated the developmental processes of CVP and VEG at these developmental stages. At E16 and PN3, photos were taken of the serial frontal sections, stained by pan-Cytokeratins, from the anterior to the posterior of the CVP and VEG under microscopy and then reconstructed using the "Image-J" reconstruction program (Figs. 1, 2). Epithelial tissues of the CVP and VEG, shown with the pan-Cytokeratins positive localizations, were presented in gray and combined by a computer program. After 3D reconstructions, we examined the detailed structure of the CVP at E16, shown with the round bracket-like structures (Fig. 1B). Interestingly, the invaginated epithelium of the CVP was seen in both lateral sides of the CVP, but not in the anterior or posterior parts of the CVP. Viewed from the bottom, these specific pattern formations of invaginated epithelium of the CVP were

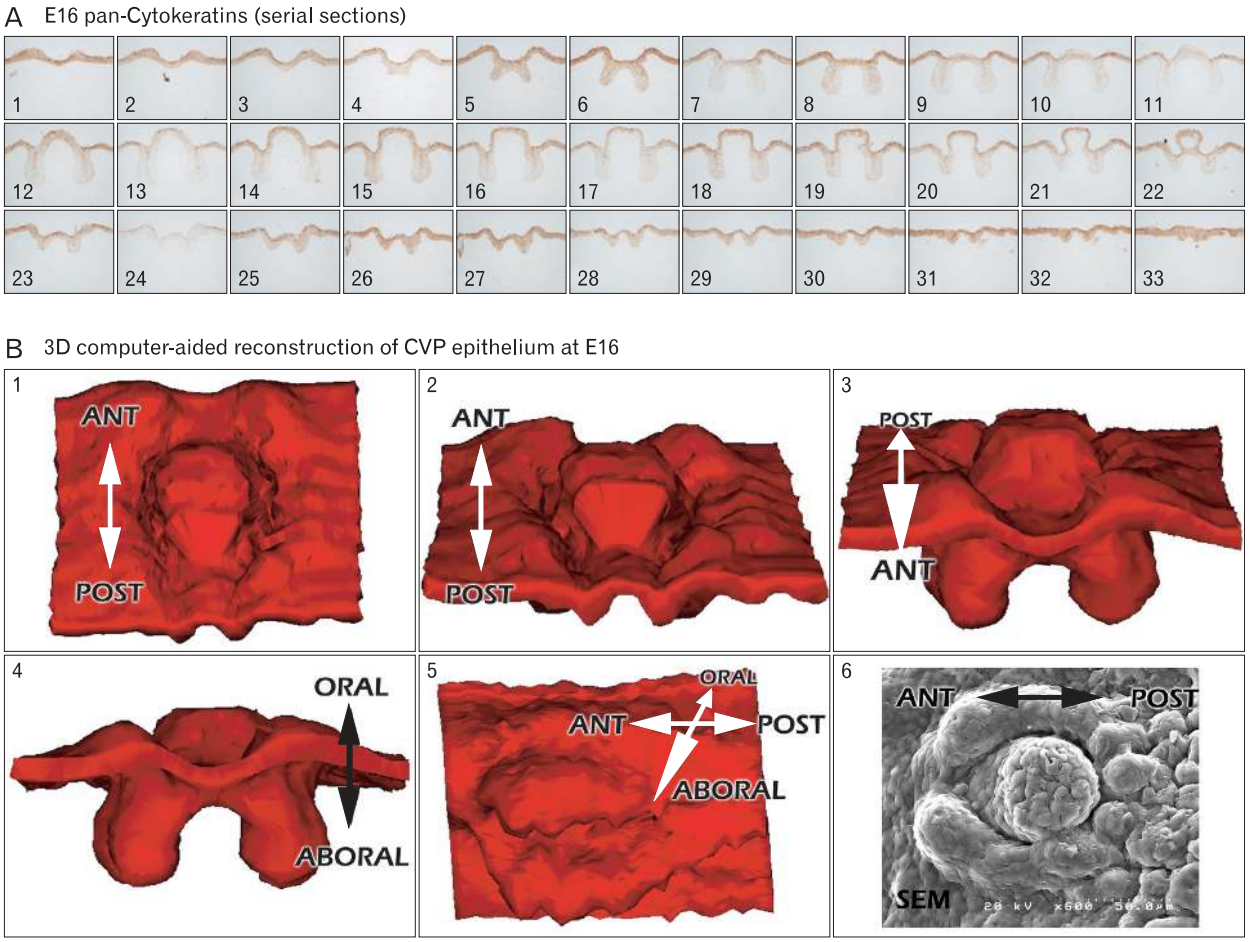

Fig. 1. Three-dimensional (3D) computer-aided reconstruction after pan-Cytokeratins (pan-Cks) immunostaining of circumvallate papilla (CVP) at embryonic day 16 (E16). (A) Serial frontal sections after pan-Cks immunohistochemistry. The number on each slide indicates the the order of slide from anterior to posterior. Gray colors demarcate the pan-Cks positive epithelial tissues. (B1-5) 3D computer-aided reconstruction of CVP epithelium at E16. Gray colors indicate the positive cells of pan-Cks. (B6) Scanning electron microscopic (SEM) observations of E16 CVP. ANT, anterior; POST, posterior.

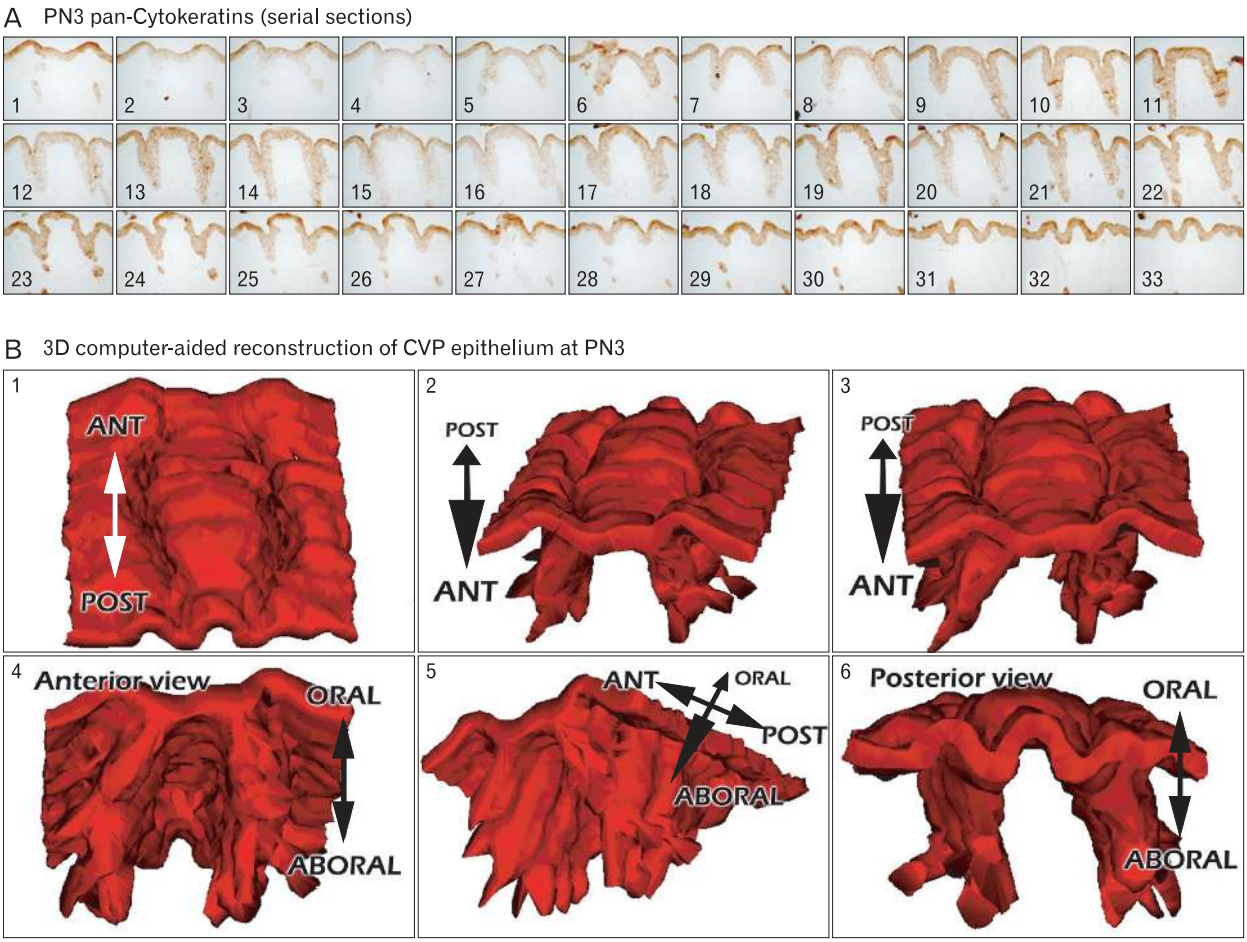

Fig. 2. Three-dimensional (3D) computer-aided reconstruction after pan-Cytokeratins (pan-Cks) immunostainings of circumvallate papilla (CVP) at postnatal day 3 (PN3). (A) Serial frontal sections after the pan-Cks immunohistochemistry. The number on each slide indicates the order of slide from anterior to posterior. Gray colors demarcate the pan-Cks positive epithelial tissues. (B) 3D computer-aided reconstruction of CVP epithelium at PN3 is presented, with the gray color indicating the positive cells of pan-Cks. ANT, anterior; POST, posterior.

confirmed (Fig. 1B5). Ultra-structural observations using scanning electron microscope (SEM) were performed using a littermate to evaluate the similarity and accuracy of 3D reconstructions (Fig. 1B6). These results showed high fidelity of the 3D computer-aided reconstruction method in defining the detailed structures of developing organs. At PN3, the CVP showed a larger size with the extension along the anteroposterior axis than those of E16 (Fig. 2). In addition, the initiation of branching formation to form the VEG was examined at PN3 (Fig. 2A). In particular, the invaginated epithelia in the lateral trench wall showed the specific branching patterning with the bifurcation along the lateral and middle directions (Fig. 2B).

Localization patterns of cell proliferation and nerve innervations

We examined the precise localization patterns of taste bud formation and nerve innervation patterns in the CVP and VEG using UEA1 and PGP9.5 (Fig. 3). At 8 weeks, adult specimens showed the positive localization patterns of UEA1, a well known marker for detecting taste buds (Fig. 3A, B) [23]. UEA1 positive cells were examined only in the epithelium of the taste buds in the trench lateral wall of the CVP. Localization patterns of PGP9.5, which showed the localizations of peripheral nerves, were detected in the mesenchymal cores of the CVP and the lateral trench walls of both lateral sides (Fig. 3C, D). Based on these specific localization patterns of UEA1 for taste buds, we concluded that PGP9.5 was not sufficient for evaluating the detailed function of nerve innervations in taste bud formation. For

http://dx.doi.org/10.5115/acb.2011.44.4.274

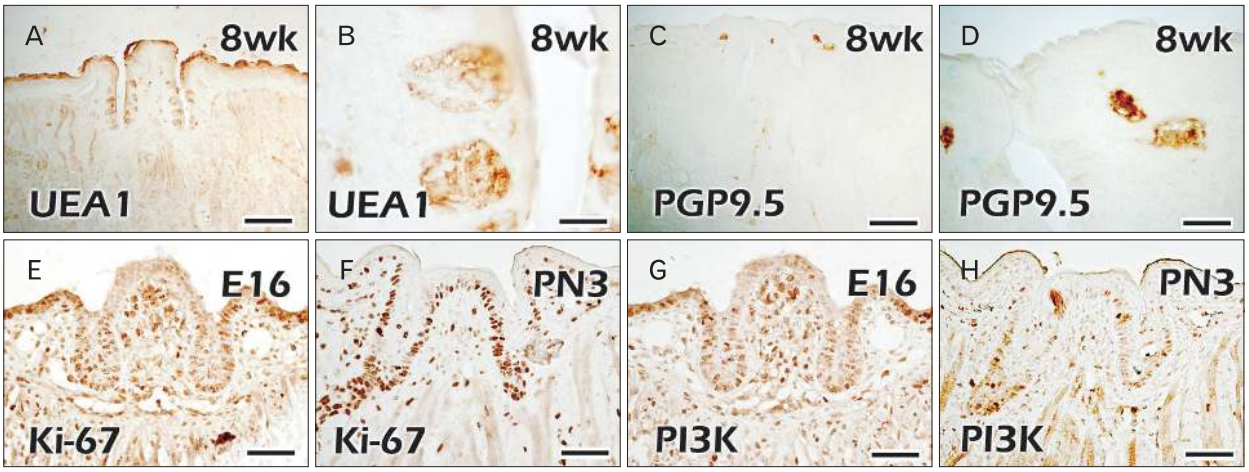

Fig. 3. Immunostaining of circumvallate papilla (CVP) and von Ebners' gland (VEG) using various markers for taste buds, nerves, and cell proliferation. (A, B) Specific localization patterns of Ulex europaeus agglutinin 1 (UEA1) in the taste bud regions of CVP epithelium in adult mice. (C, D) PGP9.5 localization patterns in the mesenchymal core regions of apex part of CVP in adult mice. (E, F) Cell proliferations occur mainly in the VEG forming regions of CVP epithelium at embryonic day 16 (E16) and postnatal day 3 (PN3). (G, H) Phosphoinositide 3-kinase (PI3K), a well-known mediator in the receptor tyrosine kinase pathway, localizes in the VEG forming epithelium at E16 and PN3. Scale bars=500 μm (A, C), 20 μm (B, D), 50 μm (E-H).

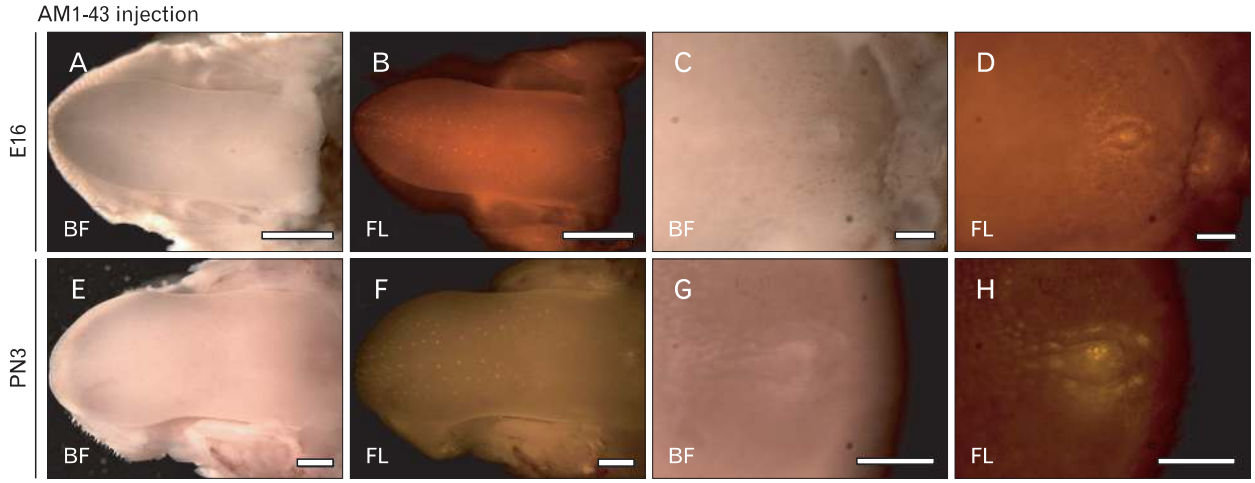

Fig. 4. Whole mount observations of AM1-43 microinjected tongues. (A-D) Twenty-four hour after *the in utero* injections of AM1-43, positive localizations are detected in the circumvallate papilla (CVP) and fungiform papillae regions. (E-H) After intra-peritoneal injections of AM1-43 for 24 h, fungiform papillae and CVP show much stronger positive reactions of AM1-43 than those of embryonic day 16 (E16). PN3, postnatal day 3; BF, bight field; FL, fluorescent. Scale bars=1 mm (A, B, E, F), 250 μm (C, D), 500 μm (G, H).

examination of cellular mechanisms besides nerve innervations, we examined the localization patterns of cell proliferation using immunostaining of Ki-67 and PI3K at E16 and PN3 (Fig. 3E-H). At E16, strong positive localizations of Ki-67 were observed only in the epithelium of the lateral trench wall of the CVP, except in the apex part (Fig. 3E). Interestingly, PI3K showed the similar localization patterns of positive epithelial cells to those of Ki-67 at E16 (Fig. 3G). Mesenchymal core regions underlying the apex part of the CVP showed the stronger positive reactions of Ki-67 and PI3K at E16 (Fig. 3E, G). These coinciding localizations of Ki-67 and PI3K suggest that cell proliferation through the PI3K activity would play roles in CVP morphogenesis. At PN3, as was observed in the previous report, specific strong localization patterns of Ki-67 and PI3K were observed in the stalk part of the CVP epithelium, where a branching formation of the VEG would be initiated (Fig. 3F, H) [4].

Microinjections of AM1-43 and its evaluations

In utero and intraperitoneal injections of AM1-43 were performed at E15 and PN2 for 24 hours to evaluate the terminal end of nerves during CVP and VEG formation (Fig. 4). Since the AM1-43, a nontoxic, fluorescent, cationic dye of which the fluorescence increases many times after partitioning into the membrane, has been widely used to observe synaptic vesicle recycling [24]. Twenty-four hours

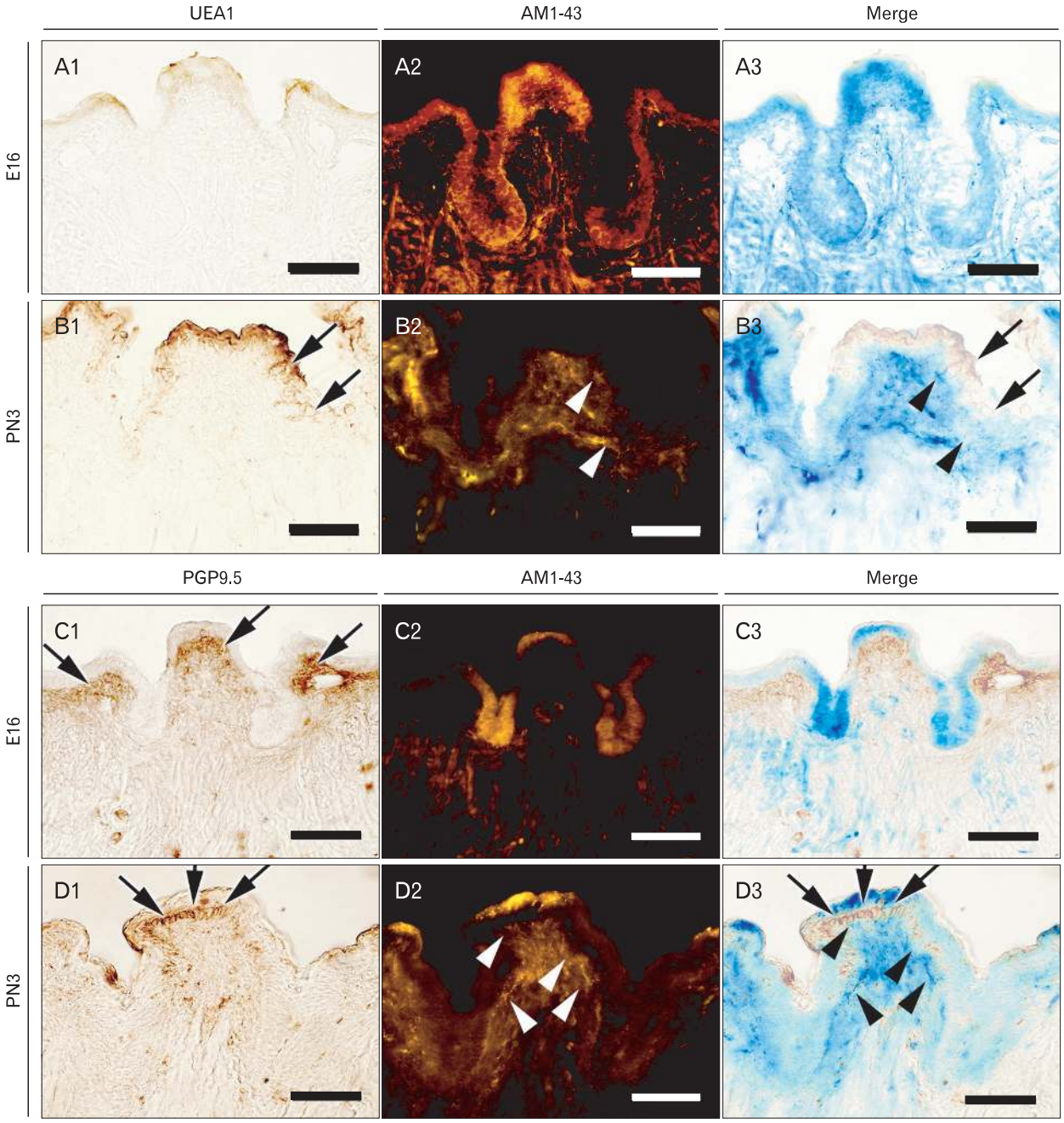

Fig. 5. Analysis of co-localization patterns of AM1-43 with Ulex europaeus agglutinin 1 (UEA1) and PGP9.5. After AM1-43 observations using frontal frozen sections, immunostaining was examined using UEA1 and PGP9.5, respectively. (A1-3) At embryonic day 16 (E16), (B1-3) at postnatal day 3 (PN3), co-localization patterns are examined between AM1-43 and UEA1. (C1-3) At E16, (D1-3) at PN3, co-localization patterns are examined between AM1-43 and PGP9.5. (A1, B1, C1, D1) Immunostaining results, (A2, B2, C2, D2) fluorescent observations of AM1-43, (A3, B3, C3, D3) merged figures. Arrows indicate positive reactions of markers and arrow heads indicate positive localization patterns of AM1-43. Scale bars=50 μm.

http://dx.doi.org/10.5115/acb.2011.44.4.274

after the *in utero* injections of AM1-43 at E15, tongues showed normal E16 tongue morphology (Fig. 4A, C). At E16, positive fluorescent reactions of AM1-43 were visualized in the apex part of the fungiform paipillae with the stereotypic pattern formation (Fig. 4B). The lateral trench wall and the apex part of the CVP showed the specific positive localization patterns of AM1-43 in the posterior part of the tongue (Fig. 4D). Twenty-four hours after the intraperitoneal injections of AM1-43 at PN2, the similar localization patterns of AM1-43 to those of E16 were observed (Fig. 4E-H). Especially, the CVP showed significantly stronger localization patterns of AM1-43 in the apex area than those of E16 (Fig. 4H).

After the microinjections of AM1-43, frontal sections were performed to evaluate the efficiency of AM1-43 in detecting the nerve innervations and the relationships among nerve innervations, taste buds formation of the CVP, and the branching formation of the VEG (Fig. 5). We examined the localization patterns of UEA1 and AM1-43 in the same slide; it was possible to evaluate the co-localization patterns of two markers with accuracy. At E16, there was no evidence of a positive reaction of UEA1 in developing the CVP (Fig. 5A1). Epithelial localization patterns of AM1-43 were observed in the apex and lateral trench wall regions of the CVP (Fig. 5A2). At PN3, UEA1 showed the broad localization patterns of taste bud forming regions in the lateral trench wall region of the CVP epithelium (Fig. 5B1). Specified and strong localization patterns of AM1-43 were examined underneath the CVP lateral trench wall epithelium (Fig. 5B2). After merging of the UEA1 and AM1-43, we found the similar localization patterns of two markers at PN3 (Fig. 5B3). The strong localization patterns of mesenchymal PGP9.5 were only examined in the mesenchyme underlying the apex part of CVP at E16 and PN3 (Fig. 5C1, D1). However, at E16, the localization patterns of AM1-43 were examined in the apex and VEG, forming epithelial cells (Fig. 5C3). At PN3, AM1-43 showed the differential and gradual localization patterns in the mesenchymal cells of CVP, where the taste buds and branch morphogenesis of VEG would be initiated (Fig. 5D2, D3). After merging the two markers at PN3, we could observe the differential localization patterns of AM1-43 and PGP9.5 (Fig. 5C3).

Discussion

In this study, we examined the detailed developmental processes forming the CVP and VEG structures. In particular, successive developmental processes for forming the CVP and VEG were evaluated using detailed morphological approaches including a 3D computer-aided reconstruction method and immunostaining with various markers. In addition, AM1-43, a fixable, activity-dependent fluorescent nerve terminal probe, was microinjected at E15 and PN2 for 24 hours to evaluate the relationship between nerve innervations and CVP/VEG development. AM1-43 is a useful tool for synapse studies where subsequent fluorescent immunohistochemistry is desired. Based on these results, we could examine the detailed morphological evidence in CVP and VEG development.

Morphological evaluations using the 3D computer-aided reconstruction

3D reconstruction methods are classic and canonical methods in the histology field to define the detailed structure of specific organs. Abundant cutting-edge techniques are available to examine detailed morphological structures, including micro-computed tomography and confocal microscopy. However, these methods incur a higher performance cost with expensive equipment. Therefore, we attempted to evaluate the specific structure of developing CVP and VEG using a 3D computer-aided reconstruction method, which has commonly been used in other anatomical and histological fields [25]. Serial histological sections with immunostaining and aligning using the software *Image-j* allowed definition of the fine structures of CVP and VEG complex in mice embryogenesis. At E16, cradle-like structures of epithelial invaginations were shown using pan-Cytokeratin immunostainings after frontal serial sections (Figs. 1, 2). The specific structure of E16 CVP coincided with ultrastructural observations using SEM (Fig. 1). These invaginated epithelial tissues at E16 will develop to form the VEG through cell proliferation [4]. In this study, we also evaluated the accuracy of 3D computer-aided reconstruction method using a comparison with ultrastructural examinations (Fig. 1). Reconstructed structures of CVP almost coincided with SEM results. This 3D computer-aided reconstruction method can be applied to other organogeneses to understand the dynamic epithelial differentiation and morphogenesis. At PN3, which showed the most dramatic alteration patterns in CVP and VEG development, invaginated epithelia showed specific bifurcation patterns along the linguobuccal direction (Fig. 2). These specific morphological alterations of branching formation suggest that mesenchymal factors

might play crucial roles in the pattern formation of epithelial invaginations, as seen in the lung branching formation [26]. During development, many organs, including the kidney, lung, and mammary gland, need to branch in a regulated manner to be functional [27]. Multicellular branching involves changes in cell shape, proliferation, and migration.

Epithelial morphogenesis accompanying the nerve innervations

A previous report showed the localization patterns of PGP9.5 in CVP and VEG development [9]. However, these simple localization patterns did not explain the detailed function of nerve innervations in CVP and VEG formation. In addition, although molecular interactions have reported that the future taste bud forming regions in the CVP epithelium can be determined by signaling regulations between Wnt11 and Shh [4], this report could not give a detailed description of taste bud formation. For a long time, this lack of a detailed answer became a criticism of the subsequent relationship of nerve innervations and morphologic changes in the period of taste buds development of CVP and the branching formation of VEG. To answer these questions of morphogenesis, developing CVP and VEG were examined using the pan-neuronal antibody, PGP9.5, directed against ubiquitin carboxyl terminal hydrolase. In addition, we examined the specific localization patterns of UEA1, which binds specifically to glycoproteins and glycolipids in endothelial cells, as a marker for taste buds (Fig. 3). In adult mice, UEA1 was localized in the taste bud area, but PGP9.5 was not sufficient to define the localizations of nerve endings (Fig. 3). Based on these results, we decided to use a better marker for detecting nerve innervations with an activity-dependent manner. A previous report revealed that epithelial cell proliferation could be a key mechanism for epithelial invaginations to form the CVP and VEG structures [4]. In addition, PI3K is a well-known mediator in the receptor tyrosine kinase pathway for various cellular events, including proliferations [28]. Restricted localization patterns of Ki-67 and PI3K in the VEG forming epithelium suggest that cell proliferation via the PI3K pathway plays important roles in taste bud formation and VEG development. Based on the restricted and strong cell proliferations in VEG forming epithelium, we suggest that positioning taste buds by cell proliferation could be a factor to induce the nerve innervations in the CVP mesenchymal regions.

To define the precise relationship between nerve innervations and taste bud formation of CVP and the branching formation of VEG, we performed microinjections of AM1-43 at E15 and PN2, then observed them after 24 hours. AM1-43, a well-known nerve terminal probe, was the best candidate molecule to define the precise localizations of nerve endings in an activity dependent manner. When we attempted to perform the microinjection of AM1-43 intraperitoneally in the pregnant mice at E15, it was impossible to detect the positive reactions of AM1-43 with any accuracy (data not shown). This result is due to the placenta-blood barrier. To permit the penetration of AM1-43 in developing embryos, we employed the *in utero* injection methods [20-22]. Twenty-four hours after microinjection of AM1-43, we found interesting localization patterns of AM1-43 in the apex parts of fungiform papillae and CVP at E16 and PN3 (Fig. 4). Particularly, the CVP forming regions showed specific and strong localization patterns of AM1-43 with the apex parts of the lateral trench walls and CVP at E16 and PN3 (Fig. 4).

To investigate the detailed localization patterns of AM1-43, frontal frozen sections were performed and immunostained using UEA1 and PGP9.5. The localization patterns of UEA1 and PGP9.5 at E16 and PN3 were examined using the same slides, and the AM1-43 injections were performed one day prior to the examinations (Fig. 5). At E16, *in utero* injected AM1-43 was localized mainly in the invaginated epithelium of CVP and was shown with broad patterns in the apex epithelial area of CVP. Normally, AM1-43, a vital fluorescent dye, enters sensory cells and neurons through ion channels and open mechanotransduction channels. AM1-43 can also enter cells by endocytosis [24]. At E16, epithelial localizations of AM1-43 can be explained by physiological processes of epithelial cells, including endocytosis, membrane trafficking, and exocytosis. At PN3, mesenchymal localization patterns of AM1-43 were examined with the gradual positive reactions and in an activity dependent manner. At E16, UEA1, a well-known marker for taste bud differentiation, did not show any positive reactions in the CVP forming epithelium. However, UEA1 was observed in the contour of the taste bud forming regions in the CVP epithelium at PN3. At PN3, positive reactions of AM1-43 in the epithelium were co-localized with the strongest epithelial UEA1 localizations. These results imply that nerve innervations have a relationship with the formation of taste buds (Fig. 5B3). Localization patterns of PGP9.5 were restricted in the apex mesenchyme underlying epithelium at E16 and PN3. Compared with the PGP9.5, AM1-43 localizations were significantly broader in the CVP

http://dx.doi.org/10.5115/acb.2011.44.4.274

mesenchyme. However, differential and gradual levels of AM1-43 positive reactions were examined in an activity dependent manner.

In this study, we examined the precise morphological changes of CVP and VEG using the 3D computer-aided reconstruction method during mice embryogenesis. These unique morphological changes in CVP and VEG formation with the cellular events including nerve innervations and cell proliferation can provide an insightful model for the study of patterning and cell-differentiation during organogenesis. In addition, these prevailing differentiation mechanisms in CVP and VEG involved in epithelial development are of importance in tissue engineering and regeneration in regulating epithelial tissue formation.

Acknowledgements

This work was supported by the National Research Foundation of Korea (NRF) grant funded by the Korea government (MEST) (No. 2009-0073808).

References

1. Jung HS, Akita K, Kim JY. Spacing patterns on tongue surface-gustatory papilla. Int J Dev Biol 2004;48:157-61.
2. Spielman AI, D'Abundo S, Field RB, Schmale H. Protein analysis of human von Ebner saliva and a method for its collection from the foliate papillae. J Dent Res 1993;72:1331-5.
3. Sbarbati A, Crescimanno C, Merigo F, Benati D, Bernardi P, Bertini M, Osculati F. A brief survey of the modifications in sensory-secretory organs of the neonatal rat tongue. Biol Neonate 2001;80:1-6.
4. Kim JY, Lee MJ, Cho KW, Lee JM, Kim YJ, Jung HI, Cho JY, Cho SW, Jung HS. Shh and ROCK1 modulate the dynamic epithelial morphogenesis in circumvallate papilla development. Dev Biol 2009;325:273-80.
5. Fujimoto S, Murray RG. Fine structure of degeneration and regeneration in denervated rabbit vallate taste buds. Anat Rec 1970;168:383-413.
6. Field RB, Dromy R, Hand AR. Regulation of secretion of enzymes from von Ebner's gland of rat tongue. J Dent Res 1987; 66:586-7.
7. Sbarbati A, Crescimanno C, Osculati F. The anatomy and functional role of the circumvallate papilla/von Ebner gland complex. Med Hypotheses 1999;53:40-4.
8. Sbarbati A, Merigo F, Bernardi P, Crescimanno C, Benati D, Osculati F. Ganglion cells and topographically related nerves in the vallate papilla/von Ebner gland complex. J Histochem Cytochem 2002;50:709-18.
9. Jitpukdeebodintra S, Chai Y, Snead ML. Developmental patterning of the circumvallate papilla. Int J Dev Biol 2002;46:755-63.
10. Mbiene JP, Roberts JD. Distribution of keratin 8-containing cell clusters in mouse embryonic tongue: evidence for a prepattern for taste bud development. J Comp Neurol 2003;457:111-22.
11. Taniguchi R, Shi L, Honma S, Fujii M, Ueda K, El-Sharaby A, Wakisaka S. Localization of Ulex europaeus agglutinin-I (UEA-I) in the developing gustatory epithelium of the rat. Arch Histol Cytol 2004;67:187-93.
12. Lee MJ, Kim JY, Lee SI, Sasaki H, Lunny DP, Lane EB, Jung HS. Association of Shh and Ptc with keratin localization in the initiation of the formation of circumvallate papilla and von Ebner's gland. Cell Tissue Res 2006;325:253-61.
13. Seta Y, Kataoka S, Toyono T, Toyoshima K. Immunohistochemical localization of aromatic L-amino acid decarboxylase in mouse taste buds and developing taste papillae. Histochem Cell Biol 2007;127:415-22.
14. Fukami H, Bradley RM. Biophysical and morphological properties of parasympathetic neurons controlling the parotid and von Ebner salivary glands in rats. J Neurophysiol 2005; 93:678-86.
15. Takeda M, Suzuki Y, Obara N, Uchida N, Kawakoshi K. Expression of glial cell line-derived neurotrophic factor (GDNF) and GDNF family receptor alpha1 in mouse taste bud cells after denervation. Anat Sci Int 2005;80:105-10.
16. Suwabe T, Fukami H, Bradley RM. Synaptic responses of neurons controlling the parotid and von Ebner salivary glands in rats to stimulation of the solitary nucleus and tract. J Neurophysiol 2008;99:1267-73.
17. Cheng SJ, Huang CF, Chen YC, Lee JJ, Chang HH, Chen HM, Chiang ML, Kuo MY, Kok SH, Tseng CY. Ultrastructural changes of posterior lingual glands after hypoglossal denervation in hamsters. J Anat 2009;214:163-70.
18. Kim M, Chiego DJ Jr, Bradley RM. Morphology of parasympathetic neurons innervating rat lingual salivary glands. Auton Neurosci 2004;111:27-36.
19. Shiraishi M, Doi Y, Kayashima K, Fujimoto S. Antioxidant enzyme immunoreactivity in rat von Ebner gland after nickel treatment. Med Mol Morphol 2008;41:44-52.
20. Stickrod G. In utero injection of rat fetuses. Physiol Behav 1981; 27:557-8.
21. Itah R, Gitelman I, Tal J, Davis C. Viral inoculation of mouse embryos *in utero*. J Virol Methods 2004;120:1-8.
22. Nishikawa S. Histochemistry of nerve fibres double labelled with anti-TRPV2 antibodies and sensory nerve marker AM1-43 in the dental pulp of rat molars. Arch Oral Biol 2008;53:859-64.
23. Wakisaka S. Lectin histochemistry of taste buds in the circumvallate papilla of the rat. Chem Senses 2005;30 Suppl 1:i46-7.
24. Meyers JR, MacDonald RB, Duggan A, Lenzi D, Standaert DG, Corwin JT, Corey DP. Lighting up the senses: FM1-43 loading of sensory cells through nonselective ion channels. J Neurosci

2003;23:4054-65.
25. Kim JN, Koh KS, Lee E, Park SC, Song WC. The morphology of the rat vibrissal follicle-sinus complex revealed by three-dimensional computer-aided reconstruction. Cells Tissues Organs 2011;193:207-14.
26. Freem LJ, Escot S, Tannahill D, Druckenbrod NR, Thapar N, Burns AJ. The intrinsic innervation of the lung is derived from neural crest cells as shown by optical projection tomography in Wnt1-Cre;YFP reporter mice. J Anat 2010;217:651-64.
27. Mailleux AA, Tefft D, Ndiaye D, Itoh N, Thiery JP, Warburton D, Bellusci S. Evidence that SPROUTY2 functions as an inhibitor of mouse embryonic lung growth and morphogenesis. Mech Dev 2001;102:81-94.
28. Cho KW, Cho SW, Lee JM, Lee MJ, Gang HS, Jung HS. Expression of phosphorylated forms of ERK, MEK, PTEN and PI3K in mouse oral development. Gene Expr Patterns 2008;8:284-90.